

Strong dependence of the interlayer coupling on the hole mobility in antiferromagnetic $\text{La}_{2-x}\text{Sr}_x\text{CuO}_4$ ($x < 0.02$)

M. Hücker,^{1,4} H.-H. Klauss,² and B. Büchner³

¹Physics Department, Brookhaven National Laboratory, Upton, New York 11973, USA

²Metallphysik und Nukleare Festkörperphysik, TU-Braunschweig, 38106 Braunschweig, Germany

³Institut für Festkörper- und Werkstofforschung Dresden, D-01171 Dresden, Germany

⁴II. Physikalisches Institut, Universität zu Köln, 50937 Köln, Germany

(Received 12 August 2004; published 29 December 2004)

We have studied the magnetic coupling between the CuO_2 planes in the antiferromagnetic (AF) phase of Sr- and Zn-doped La_2CuO_4 by analyzing the spin-flip transition in the magnetization curves. We find that the interlayer coupling plays a key role in the suppression of the AF phase, and that only mobile holes cause a strong frustration of the interlayer coupling. Depending on the hole mobility, samples with identical Néel temperature can have a very different interlayer coupling.

DOI: 10.1103/PhysRevB.70.220507

PACS number(s): 74.25.Ha, 74.72.Dn, 75.30.Hx, 75.40.Cx

All cuprate high-temperature superconductors are characterized by a layered crystal structure. Key elements of this structure are the CuO_2 planes which are a prototype of a spin $S=1/2$ two-dimensional (2D) Heisenberg antiferromagnet. Insulating CuO_2 planes, such as those in undoped La_2CuO_4 , exhibit a three-dimensional antiferromagnetic (3D AF) order, while CuO_2 planes doped with hole-like charge carriers, as those in $\text{La}_{2-x}\text{Sr}_x\text{CuO}_4$, become superconducting.¹ Both phenomena, antiferromagnetic order as well as superconductivity, depend on a finite electronic coupling between the planes.² In this paper we focus on the doping dependence of the interlayer coupling in the AF phase of lightly Sr-doped La_2CuO_4 .

In $\text{La}_{2-x}\text{Sr}_x\text{CuO}_4$ the 3D AF order is destroyed by a remarkably small amount of 2% holes ($x=0.02$), which is in sharp contrast to $\sim 41\%$ in the case of the substitution of Cu with nonmagnetic Zn.^{1,3} Since the suppression of the 3D AF order by holes is a precondition for the occurrence of superconductivity, great efforts have been made to map each stage of this process.^{1,4-6} The Néel temperature T_N decreases from 325 K for $x=0$ to about 80 K for $x=0.019$ and then drops to zero at $x=0.02$.^{1,6} At the same time for $x \geq 0.008$ the so-called spin freezing regime evolves at temperatures $T \lesssim 30$ K.^{4,5} At $x=0.02$ this regime crosses over to the so-called cluster spin-glass phase, which reaches into the superconducting phase that appears at $x=0.06$.¹ Recent neutron-diffraction experiments indicate that the spin freezing regime and the spin-glass phase are closely related.⁷ In both phases an incommensurate spin modulation was observed.^{7,8} Various models were suggested to describe the suppression of the AF order in $\text{La}_{2-x}\text{Sr}_x\text{CuO}_4$.⁹⁻¹² The frustration model assumes that individual localized holes cause a frustration of the in-plane and the interlayer coupling.⁹ In the finite-size scaling model holes segregate into domain walls which limit the 2D correlation length $\xi_{2D} \propto \sqrt{T_N}$.^{5,10}

To find out the primary controlling parameter for the suppression of the 3D AF order in $\text{La}_{2-x}\text{Sr}_x\text{CuO}_4$, we have studied the magnetic interlayer coupling J_{\perp} as a function of Sr and/or Zn doping. Zn doping is used to reduce the mobility of the holes and to introduce spin vacancies.⁶ As J_{\perp} is about

five orders of magnitude weaker than the Cu-O-Cu in-plane superexchange of $J=135$ meV, it is not possible to measure it by neutron scattering. Instead, we have determined J_{\perp} from the spin-flip transition which can be induced for $H \parallel c$ due to the Dzyaloshinsky-Moriya Cu-spin canting.¹³ Our analysis of this transition shows that only mobile holes cause a drastic suppression of the interlayer coupling. Codoping with Zn recovers an interlayer coupling nearly as strong as in pure La_2CuO_4 due to the localization of the holes. Most remarkably, samples with identical hole concentration and similar T_N can have a very different interlayer coupling, depending on the mobility of the holes.

The dc magnetization $M(H)$ of five polycrystals $\text{La}_{2-x}\text{Sr}_x\text{Cu}_{1-z}\text{Zn}_z\text{O}_4$ (Table I) was measured with a vibrating-sample magnetometer (VSM) with $T_{max}=290$ K and $H_{max}=14$ T. Samples were annealed in vacuum (1/2 h, 800 °C), their synthesis is described in Ref. 6.

La_2CuO_4 exhibits a collinear spin structure with spins nearly parallel to the b axis.¹³ However, in the low-temperature orthorhombic (LTO) phase of La_2CuO_4 the CuO_6 octahedra are tilted, which allows for Dzyaloshinsky-Moriya (DM) superexchange. As a consequence, nearest-neighbor Cu spins are slightly canted, which results in small moments $M_{DM} \parallel c$.¹³ Below T_N the DM moments of adjacent planes are AF ordered, but can be ferromagnetically aligned in an external magnetic field $H \parallel c$.¹³ The spin flip (SF) takes place when H acting on the AF ordered part of the DM moment M_{DM}^{AF} overcomes the interlayer coupling (left inset

TABLE I. Studied $\text{La}_{2-x}\text{Sr}_x\text{Cu}_{1-z}\text{Zn}_z\text{O}_4$ samples (see text).

Sr	Zn	T_N (K)	H_{SF} (T)	M_{DM}^{AF} [$10^{-3}(\mu_B/\text{Cu})$]	J_{\perp} (μeV)
0	0	312	4.5(5)	2.7(3)	2.9(5)
0.011	0	222	3.6(3)	2.1(3)	1.7(5)
0.017	0	132	2.4(2)	1.2(2)	0.7(3)
0.017	0.10	134	3.9(4)	3.0(3)	2.7(5)
0	0.15	166	3.6(4)	3.4(3)	2.7(5)

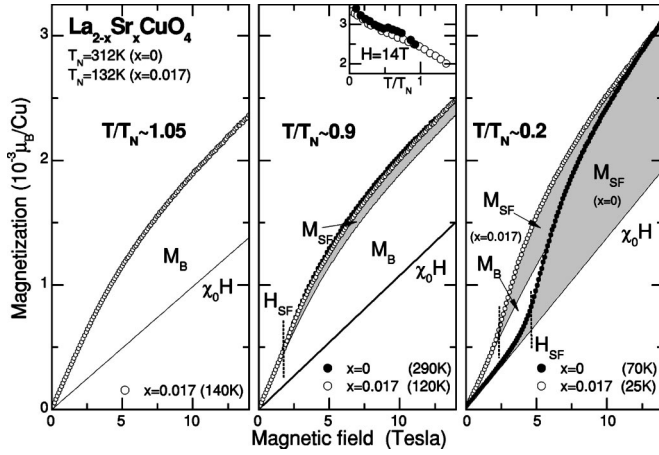


FIG. 1. Magnetization curves $M(H)$ of $\text{La}_{2-x}\text{Sr}_x\text{CuO}_4$ with $x=0$ and $x=0.017$ at reduced temperatures $T/T_N=1.05, 0.9$, and 0.2 (see text). In the left panel only data for $x=0.017$ is shown since $1.05 \times T_N$ for $x=0$ is above the maximum temperature of our VSM (290 K).

Fig. 2). Once $M_{DM}^{AF}(T)$ and the spin-flip field $H_{SF}(T)$ have been extracted from the $M(H)$ curves, the interlayer coupling J_{\perp} can be calculated from the low-temperature limit,¹³

$$M_{DM}^{AF}(0)H_{SF}(0) \approx S^2 J_{\perp}. \quad (1)$$

The analysis is complicated by the fact that the DM moments, which are of the order of $\sim 10^{-3} \mu_B/\text{Cu}$, cause the $M(H)$ curves to be nonlinear in the AF phase as well as in the paramagnetic phase.^{13,14} As an example we show in Fig. 1, $M(H)$ of La_2CuO_4 ($T_N=312$ K) and $\text{La}_{1.983}\text{Sr}_{0.017}\text{CuO}_4$ ($T_N=132$ K) as a function of the reduced temperature T/T_N . In the paramagnetic phase ($T/T_N > 1$) the nonlinear contribution can be described by a term M_B which contains a Brillouin function for spin $S=1/2$ (details below). In the AF phase ($T/T_N < 1$) the nonlinear contribution is always a combination of M_B and a term M_{SF} which arises from the spin flip

$$M = \begin{cases} \chi_0 H + M_B & (T > T_N) \\ \chi_0 H + M_B + M_{SF} & (T < T_N) \end{cases}, \quad (2)$$

where $\chi_0 H$ accounts for all linear terms. As one can see in Fig. 1 the spin-flip term M_{SF} is zero in the paramagnetic phase, finite but small just below T_N , and dominant at low T (gray shaded area). Furthermore, one can see that in the Sr-doped sample even at very low temperatures M_{SF} is significantly smaller than in La_2CuO_4 , while M_B is larger, which indicates the reduction of the AF order parameter by the doped holes. Clearly visible is also the smaller critical field H_{SF} for $x=0.017$.

In a single crystal the spin flip causes a steplike increase of $M(H||c)$ at $H \approx H_{SF}$ by $M_{SF} = M_{DM}^{AF}$. In a polycrystal the crystallites are oriented randomly. From integration over all directions we obtain the following field dependence of M_{SF} for $H \geq H_{SF}$:

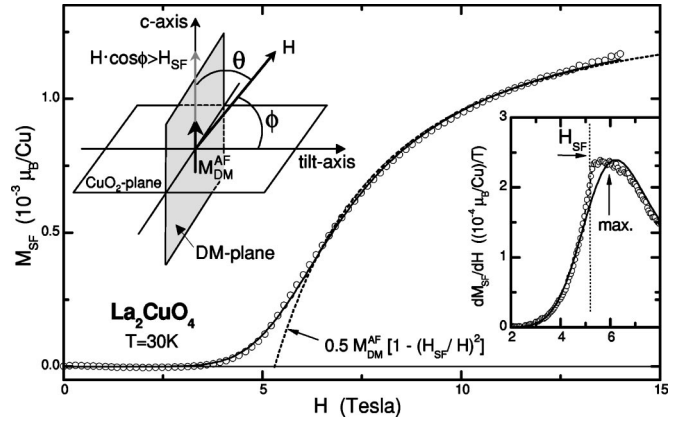


FIG. 2. Spin-flip term $M_{SF} = M - M_B - \chi_0 H$ in La_2CuO_4 at 30 K. (Dashed/Solid lines) fit according to Eq. (3) without/with Gaussian distribution of H_{SF} . Left inset: Spin flip takes place when $H \cos \theta || c$ exceeds H_{SF} . Only $M_{DM}^{AF} \cos \theta || H$ contributes to M_{SF} . Right inset: In a polycrystal $H_{SF} < H_{\max}(dM/dH)$.

$$M_{SF}(H) = \frac{1}{2} M_{DM}^{AF} [1 - (H_{SF}/H)^2]. \quad (3)$$

Obviously, in a polycrystal M_{SF} converges to $M_{DM}^{AF}/2$ for $H \rightarrow \infty$. A similar geometrical consideration for the paramagnetic phase yields the phenomenological formula for M_B ,

$$M_B(H) = M_{DM}^{NO} \int_0^{\pi/2} \tanh(kH \sin \phi) \sin^2 \phi d\phi, \quad (4)$$

where M_{DM}^{NO} is the non-AF-ordered (NO) fraction of M_{DM} per Cu spin. $k = M_{DM}^{NO} N / (k_B T + J_{\perp} N^2 S^2)$ is a phenomenological expression with $N = (\xi_{2D}/a)^2$ the number of 2D correlated Cu spins, which provides an estimate for the magnetic correlation length ξ_{2D} . ϕ is the angle between H and the tilt axis of the CuO_6 octahedra, which is normal to the DM plane (inset Fig. 2). Our analysis has shown that $M_{DM} \approx M_{DM}^{AF} + M_{DM}^{NO}$. A neglect of M_B would lead to inaccurate values for M_{DM}^{AF} , H_{SF} , and J_{\perp} , in particular when $M_B \gtrsim M_{SF}$. In the following we focus on the spin-flip term M_{SF} .

In Fig. 2 we show $M_{SF} = M - M_B - \chi_0 H$ for La_2CuO_4 at 30 K, where $M_B \approx 0$. For large H , Eq. (3) yields a good fit to the data (dashed line). Assuming a Gaussian distribution of H_{SF} in the polycrystal, integration of Eq. (3) over H_{SF} yields the solid line in Fig. 2 which perfectly fits the data in particular around H_{SF} . The extracted parameters $M_{DM}^{AF} = 2.55 \times 10^{-3} \mu_B/\text{Cu}$ and $H_{SF} = 5.2$ T are in fair agreement with $2.1 \times 10^{-3} \mu_B/\text{Cu}$ and 5.3 T for a single crystal with $T_N = 240$ K, if one takes into account the crystals lower T_N and the fact that in single crystals H_{SF} is generally 0.5–1 T larger, most likely because in polycrystals the correlation length is limited by the grain size.¹³

With the developed tools we are now able to track the temperature and doping dependence of H_{SF} , M_{DM}^{AF} , and J_{\perp} of the five studied samples (Table I). In pure La_2CuO_4 M_{DM}^{AF} increases monotonously with decreasing T , and extrapolates to $M_{DM}^{AF}(0) = 2.7 \times 10^{-3} \mu_B/\text{Cu}$ [Fig. 3(a)]. Pure Sr doping causes a drastic reduction of M_{DM}^{AF} . In contrast, in $\text{La}_2\text{Cu}_{0.85}\text{Zn}_{0.15}\text{O}_4$, though T_N is strongly reduced, at low

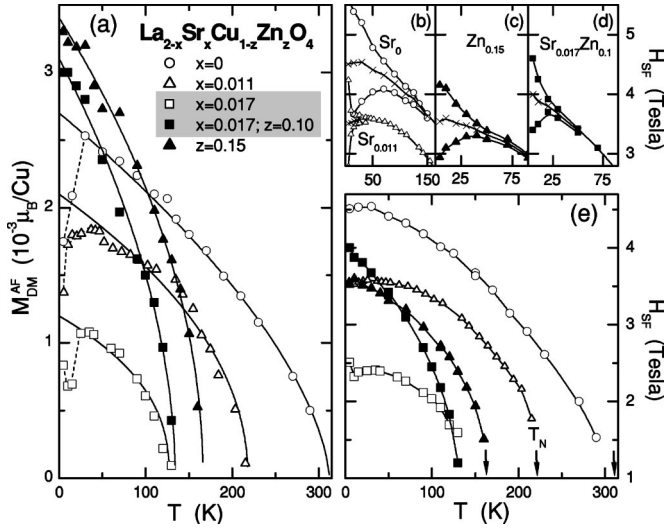


FIG. 3. Spin-flip parameters M_{DM}^{AF} (a) and H_{SF} (b)–(e) vs T in $\text{La}_{2-x}\text{Sr}_x\text{Cu}_{1-z}\text{Zn}_z\text{O}_4$. Errors in Table I. (b)–(d) H_{SF} for $dH/dt > 0$ (upper branches) and $dH/dt < 0$ (lower branches) as well as mean value (\times). (e) H_{SF} mean values.

temperatures M_{DM}^{AF} per Cu atom becomes even larger than in La_2CuO_4 . Quite remarkably, a similar behavior is observed for the Sr/Zn-codoped sample, where the twofold role of Zn is to reduce the mobility of the holes and to create spin vacancies.⁶

In La_2CuO_4 the spin-flip field H_{SF} increases with decreasing temperature and below 150 K becomes hysteretic, with its mean value (\times) saturating at 4.5 T [Figs. 3(b) and 3(e)]. Pure Sr doping strongly reduces H_{SF} as well as the hysteretic temperature range. In particular for the 1.7% Sr-doped sample only for $T \leq 10$ K a field hysteresis is observed. Both Zn-doped samples show a relatively large field hysteresis [see Figs. 3(c) and 3(d)]. Their maximum mean value for H_{SF} is smaller than in La_2CuO_4 , but in view of their low T_N , it is large when compared to H_{SF} of $\text{La}_{1.983}\text{Sr}_{0.017}\text{CuO}_4$. The specific reasons for the hysteresis effects in $\text{La}_{2-x}\text{Sr}_x\text{CuO}_4$ are not well understood. However, its distinct presence in La_2CuO_4 indicates that it is not an exclusive feature of the spin freezing regime.

As one can see in Fig. 3(a), in La_2CuO_4 and for pure Sr doping M_{DM}^{AF} decreases below 30 K. In the case of La_2CuO_4 we think that this effect is related to the large field hysteresis of the spin-flip transition, which leads to strongly distorted $M(H)$ curves and makes it difficult to extract reliable M_{DM}^{AF} values at low temperatures. In contrast, in the 1.7% Sr-doped sample M_{DM}^{AF} decreases between 30 and 15 K, where $M(H)$ is reversible and the fits of high quality. We think that, here, the effect is connected to the transition into the spin freezing regime and indicates a decrease of the AF order parameter ($\propto M_{DM}^{AF}$), which is consistent with results from neutron diffraction.⁷ Obviously, the effect is absent in both Zn-doped samples, which indicates that Zn causes a suppression of the spin freezing regime in $\text{La}_{2-x}\text{Sr}_x\text{CuO}_4$.

Following Eq. (1), we show in Fig. 4 the temperature dependence of $\mathcal{J}_\perp^* = M_{DM}^{AF} H_{SF} / S^2$, which we call the effective interlayer coupling, where H_{SF} are the mean values in Fig.

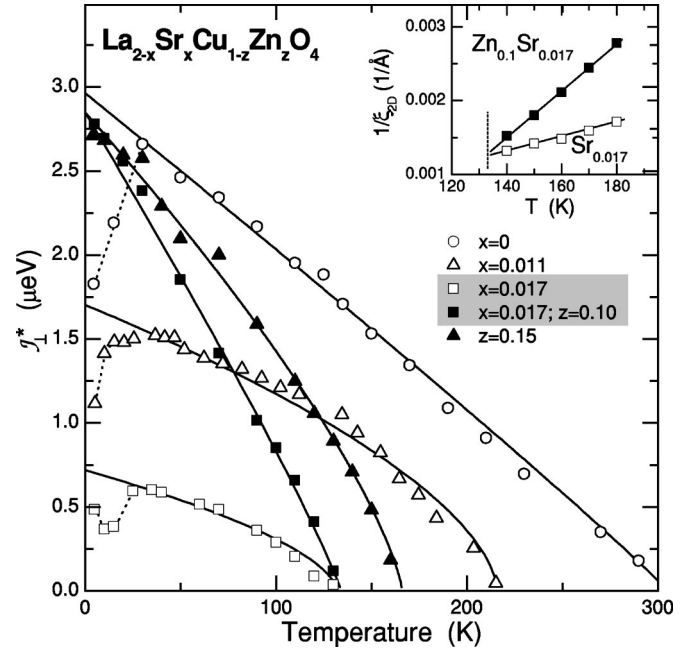


FIG. 4. Interlayer coupling in $\text{La}_{2-x}\text{Sr}_x\text{Cu}_{1-z}\text{Zn}_z\text{O}_4$. Errors in Table I. Inset: Inverse correlation length vs T for both samples with $x=0.017$. The solid lines are guides to the eye.

3(e). \mathcal{J}_\perp^* accounts for the effects of doping (x, z) and temperature and only for $T \rightarrow 0$ $\mathcal{J}_\perp^*(0) = J_\perp$, where J_\perp is the average superexchange per Cu site (Table I), although one should keep in mind that strictly speaking J_\perp is a local interaction. In La_2CuO_4 we find $\mathcal{J}_\perp^*(0) = 2.9 \mu\text{eV}$, which is in good agreement with 2.6 μeV for the single crystal mentioned above, if one takes its lower T_N but relatively high H_{SF} into account.¹³ As a function of Sr doping \mathcal{J}_\perp^* drastically decreases, and for $x=0.017$ $\mathcal{J}_\perp^*(0)$ amounts to only 25% of the value in La_2CuO_4 . In contrast, in $\text{La}_{1.983}\text{Sr}_{0.017}\text{Cu}_{0.9}\text{Zn}_{0.1}\text{O}_4$, which has exactly the same T_N , \mathcal{J}_\perp^* increases steeply below T_N and reaches nearly the same value as in La_2CuO_4 . $\text{La}_2\text{Cu}_{0.85}\text{Zn}_{0.15}\text{O}_4$ behaves similarly. The fact that in both Zn-doped samples $\mathcal{J}_\perp^*(0)$ is about the same as in La_2CuO_4 reflects Eq. (1), which says that if J_\perp is constant H_{SF} has to decrease when M_{DM}^{AF} increases [cf. Figs. 3(a) and 3(e)]. To a certain extent the 15% ($z=0.1$) and 25% ($z=0.15$) larger DM moments can be explained by an enhanced octahedra tilt angle Φ .¹⁵ Local strain around the non-Jahn-Teller-active Zn sites might amplify this effect. We emphasize that a moderate increase of the DM interaction by Zn doping only will have a small impact on J_\perp and certainly cannot explain the drastic increase by a factor of 4 observed for the two 1.7% Sr-doped samples.

Figure 4 is our major result. It shows that the mechanism for the suppression of the 3D AF order is completely different for pure hole doping (Sr) on the one hand, and nonmagnetic impurity doping (Zn) as well as Sr/Zn codoping on the other hand. In $\text{La}_{2-x}\text{Sr}_x\text{CuO}_4$ the hole mobility increases rapidly with increasing x , and just a small concentration of mobile holes strongly reduces both T_N and \mathcal{J}_\perp^* .⁶ Codoping with Zn reduces the hole mobility⁶ and causes a drastic increase of \mathcal{J}_\perp^* even if T_N is low. In particular for the two samples

with identical T_N and hole concentration x the effect of different hole mobilities is apparent.

We start the discussion by showing that individual localized holes cannot account for our observations. It is well accepted that localized holes suppress T_N much stronger than Zn, because holes are located on O sites and ferromagnetically frustrate the antiferromagnetic Cu-O-Cu exchange.⁹ In contrast, static spin vacancies do not perturb the AF order of the surrounding Cu spins.¹⁶ To see this we compare the 10% Zn- and 1.7% Sr-codoped sample with localized holes with a \sim 18% Zn-doped sample, which would have the same T_N of \sim 135 K. It immediately follows that 1.7% localized holes suppress T_N as effective as 8% Zn. Hence, the in-plane ferromagnetic frustrations of localized holes strongly reduce T_N , but hardly affect the interlayer coupling (Fig. 4). We conclude that a reduction of the interlayer coupling in $\text{La}_{2-x}\text{Sr}_x\text{CuO}_4$ is connected to a high hole mobility.

In the following we will show that our observations can be explained assuming dynamic magnetic antiphase boundaries for $T \geq 30$ K and static for $T \leq 30$ K. Evidence for static antiphase boundaries in the spin freezing regime was recently found by Matsuda *et al.*⁷ Below 30 K an incommensurate spin order was detected which coexists with the commensurate AF order. Dynamic antiphase domains were suggested¹² to explain the drastic reduction of the AF order parameter with increasing x for $30 \text{ K} < T < T_N$. Our discussion does not depend on a particular domain form or on the formation of charge stripes. What is essential is that holes are mobile, as only these holes can ferromagnetically frustrate many Cu-O-Cu-bonds and are able to excite at least antiphase boundary segments. In the presence of many of such excitations a frustration of the interlayer coupling is inevitable, as two antiphased domains in one CuO_2 -plane generally cannot AF couple simultaneously to the adjacent plane.

The drastic reduction of M_{DM}^{AF} in $\text{La}_{2-x}\text{Sr}_x\text{CuO}_4$ with increasing x for $30 \text{ K} \leq T < T_N$ can be explained by antiphase boundaries, also. Only those regions of the CuO_2 planes with AF interlayer coupling contribute to the spin flip described by M_{SF} , while in regions with frustrated interlayer coupling the magnetization of the DM moments contributes to M_B . In particular for the Sr-doped sample with $x=0.017$ the significance of M_B at low T is obvious [Fig. 1(c)]. This clearly

indicates that in $\text{La}_{2-x}\text{Sr}_x\text{CuO}_4$ with increasing x weight is shifted from M_{SF} to M_B , as the regions with AF interlayer coupling, and therefore the AF order parameter, decrease.

According to our analysis, in the 1.7% Sr-doped samples ξ_{2D} at T_N is about the same (inset Fig. 4). However, in the sample with mobile holes ξ_{2D} increases much slower with decreasing T than in the Zn-doped sample with localized holes. Hence, mobile holes seem to confine ξ_{2D} , which is consistent with the central idea of the finite-size scaling model for the temperature range $30 \text{ K} \leq T < T_N$.^{5,10} However, in this model the spin freezing regime is associated with the breakup of the domain walls when holes localize.⁵ In contrast, recent neutron-diffraction data give evidence of static magnetic domain walls in particular in the spin freezing regime.⁷

The additional reduction of M_{DM}^{AF} in the spin freezing regime can be explained in terms of a static and more even distribution of antiphase boundaries in the spin freezing regime. Since the phase of the AF correlations changes by π on crossing an in-plane antiphase boundary, a periodic arrangement of such domain walls might result in a perfect frustration of the interlayer coupling. The fact that in the Zn-doped samples no drop of M_{DM}^{AF} below $T \sim 30$ K is observed, indicates that the localization of holes by Zn destroys the incommensurate spin freezing regime and lifts the frustration of the interlayer coupling. In Ref. 11 it was suggested that Zn effectively removes frustrated in-plane bonds generated by holes. This static picture neglects that it is not favorable for a hole to go on the O site of a Cu-O-Zn bond, for Zn^{2+} has a full $3d^{10}$ shell. In contrast, resistivity data suggests that the hole mobility is reduced by impurity scattering.⁶

In summary, we have presented evidence that the drastic suppression of the antiferromagnetic phase in $\text{La}_{2-x}\text{Sr}_x\text{CuO}_4$ is associated with a magnetic decoupling of the CuO_2 planes. We concluded that the decoupling is induced by in-plane antiphase boundaries excited by mobile holes. The impact of localized holes as well as static spin vacancies on the interlayer coupling is weak.

We gratefully acknowledge helpful discussions with M. Vojta, F. Essler, and R. Konik. The work at Brookhaven was supported by the Office of Science, U.S. Department of Energy, under Contract No. DE-AC02-98CH10886.

¹C. Niedermayer *et al.*, Phys. Rev. Lett. **80**, 3843 (1998).

²N. D. Mermin and H. Wagner, Phys. Rev. Lett. **17**, 1133 (1966).

³O. P. Vajk *et al.*, Science **295**, 1691 (2002).

⁴F. C. Chou *et al.*, Phys. Rev. Lett. **71**, 2323 (1993).

⁵F. Borsa *et al.*, Phys. Rev. B **52**, 7334 (1995).

⁶M. Hücker *et al.*, Phys. Rev. B **59**, R725 (1999).

⁷M. Matsuda *et al.*, Phys. Rev. B **65**, 134515 (2002).

⁸M. Fujita *et al.*, Phys. Rev. B **65**, 064505 (2002).

⁹A. Aharony, R. J. Birgeneau, A. Coniglio, M. A. Kastner, and H. E. Stanley, Phys. Rev. Lett. **60**, 1330 (1988).

¹⁰J. H. Cho, F. C. Chou, and D. C. Johnston, Phys. Rev. Lett. **70**, 222 (1993).

¹¹I. Y. Korenblit, A. Aharony, and O. Entin-Wohlman, Phys. Rev. B **60**, R15 017 (1999).

¹²B. J. Suh *et al.*, Phys. Rev. Lett. **81**, 2791 (1998).

¹³T. Thio *et al.*, Phys. Rev. B **38**, R905 (1988).

¹⁴T. Thio and A. Aharony, Phys. Rev. Lett. **73**, 894 (1994).

¹⁵ T_{HT} of the structural transition $\text{HTT} \rightarrow \text{LTO}$ changes by 8 K/0.01 Zn and by -25 K/0.01 Sr. Hence, $M_{DM} \propto \Phi \propto [(T_{HT} - T)^{0.62}]^{1/2}$ increases by 3% ($z=0.10$) and 7% ($z=0.15$) at $T=0$ K with respect to La_2CuO_4 .

¹⁶M. Hücker and B. Büchner, Phys. Rev. B **65**, 214408 (2002), and references therein.